Eur. Phys. J. A **28**, 329–344 (2006)
DOI 10.1140/epja/i2005-10284-x

THE EUROPEAN PHYSICAL JOURNAL A

Off-shell photon light-cone wave functions with odd chirality

Ran Yu[a], Jueping Liu[b], and Kai Zhu[a]

College of Physics and Technology, Wuhan University, 430072 Wuhan, PRC[a]

Received: 19 October 2005 / Revised: 2 May 2006 /
Published online: 10 July 2006 –
Communicated by Xiangdong Ji

Abstract. Based on a more reasonable simulation method for dealing with the Λ-parameter characterizing the pole form for the form factor (the Fourier transform of the instanton zero mode), and a unified way for regularizing the integrals appearing in the expressions of the light-cone photon wave functions, the transverse photon wave function $\phi_{\gamma\perp}(u, P^2)$ at the leading twist with the on-shell or off-shell momentum have been re-examined in the effective low-energy theory derived from the instanton vacuum, and the twist-two parts of the other two photon wave functions, $h_{\gamma\|}^{(s),\text{twist two}}(u, P^2)$ and $h_{\gamma\|}^{(t),\text{twist two}}(u, P^2)$, with odd chirality are calculated based on the Wandzura-Wilczek–like relations as well. A brief discussion of the dependence of the coupling $f_\gamma^\perp(P^2)$ and the light-cone photon wave functions with respect to P^2 and the end-point behavior of the photon wave functions are given.

PACS. 11.15.Tk Other nonperturbative techniques – 12.38.Lg Other nonperturbative calculations – 11.55.Hx Sum rules – 14.70.Bh Photons

1 Introduction

The concept of the hadron light-cone wave functions distribution amplitude (momentum fractions of partons in a particular meson state) becomes more and more important since it has been firstly introduced by Brodsky and Lepage [1]. According to this concept, the effects of the underlying QCD non-perturbative dynamics are well parameterized, and proven to be very useful in the exclusive hard scattering processes [2–4]. The notion of light-cone wave functions also appears in the method of QCD light-cone sum rules [5] as the basic non-perturbative objects. The photon light-cone wave functions have the essential role, for instance, in the amplitudes for radiative hyperon decays [6], and in the power-suppressed contributions to the scattering processes of a real photon and a virtual one, such as $\gamma^*\gamma \to \pi^0$ [7], and to the deeply virtual Compton scattering [8,9].

For the pion light-cone wave function, the predicted near-asymptotic form is consistent with the analysis of the transition form factor of $\gamma^*\gamma \to \pi^0$ [7] and the corresponding measurements by the CLEO Collaboration [10]; about the photon one, however, little is known at present from experiment even at leading twist. Theoretically, its asymptotic form is fixed by the approximate conformal invariance of QCD for large virtuality [11]. An estimate to the asymptotic form is attempted by using the QCD sum rules [6], but the corresponding higher moments could not be estimated in this approach with sufficiently accuracy. As stated in ref. [12], there has been increasing evidence indicating that the conventional QCD sum rule estimates of corrections to asymptotic distribution amplitude of the photon at low scales are not reliable, so that the existing evidence in favor of the asymptotic form of the photon distribution amplitude at small virtuality of order 1 GeV is only qualitative. A discussion of the photon wave functions was also made in the constituent quark model for photon-meson transition form factors [13]. For the on-shell photon distribution amplitudes up to and including twist-four for both chirality-conserving and chirality-violating operators, a systematic classification of the two and three-particle photon wave functions is developed based on the background field formalism [12].

Nowadays, the effects of the virtual photon receive more attention due to its importance for deeply virtual Compton scattering and hard-meson production [8,9,14,15]. The off-shell forward parton distributions also appear in the factorization of the Compton amplitude in the deeply virtual domain. If one is interested in considering the corresponding correlation functions of the light-cone operators with the electromagnetic current also at space-like momentum transfer ($P^2 < 0$) or at the time-like one ($P^2 > 0$), then the off-shell photon wave functions should be taken into account.

A calculation of the photon wave functions from first principles requires a theory or a model of non-perturbative

[a] *Present address.*
[b] e-mail: jpliu@whu.edu.cn (corresponding author).

effects giving rise to a hadron structure. We choose to work in the instanton vacuum model of QCD [16]. The picture of QCD vacuum as a dilute medium of instantons leads to the formation of the gluon condensates [17,18] and of the topological susceptibility needed to cure the $U(1)$ paradox [19,20]. The instanton vacuum also explains the most important non-perturbative phenomenon of hadron structure, namely the chiral symmetry breaking. Quarks interact with the fermion zero modes of the individual instantons in the medium, and leads to the formation of a chiral condensate. If one restricts oneself to the low-energy strong interaction, the instanton vacuum model of QCD leads to a low-energy effective theory of quarks with a dynamical quark mass which drops to zero at Euclidian momenta of the order of the inverse average instanton size, $\bar{\rho}^{-1} \simeq 600\,\mathrm{MeV}$ [21].

The twist decomposition of the matrix elements for the off-shell photon parallels that for the rho meson with only one difference in isospin components [22,23], therefore, the Lorentz decomposition of the photon distribution amplitudes may be directly read off from the case of the rho meson [24]. However, this conclusion needs a concrete confirmation because the equation of motion is modified by the existence of the photon, and one may expect the appearance of some inessential new features. In our previous work [25], the Lorentz decomposition of the on- and off-shell light-cone photon distribution amplitudes is carried out up to twist four, the resultant classification of the two-particle wave functions is really similar to the rho meson with only a tiny difference in the definition of the scalar coupling, namely the denominator in the second term of the r.h.s. of eq. (16) in [25] is P^2 for the case of the virtual photon instead of μ^2 in the case of the rho meson. It should be noticed that a very important feature automatically arises in our formalism of the on- and off-shell photon wave functions, namely, when the photon momentum becomes on-shell, only the physical couplings, *i.e.*, the coupling of the transverse light-cone photon wave function of twist two, $\phi_{\gamma\perp}(u, P^2)$, to the tensor quark-antiquark non-local operator, and the coupling of the transverse light-cone wave function of twist two plus twist three, $g^{(a)}_{\gamma\perp}(u, P^2)$, to the axial quark-antiquark non-local operator, survive to be non-vanishing. All other photon wave functions, such as $h^{(t)}_{\gamma\parallel}(u, P^2)$, $h_{\gamma 3}(u, P^2)$, $h^{(s)}_{\gamma\parallel}(u, P^2)$, $\phi_{\gamma\parallel}(u, P^2)$, $g^{(v)}_{\gamma\perp}(u, P^2)$ and $g_{\gamma 3}(u, P^2)$ defined in [25], are automatically decoupled from the corresponding quark-antiquark non-local operators. This feature of the on- and off-shell light-cone photon wave functions is welcome in our present understanding and practicing of the real and virtual photons. Moreover, based on the Lorentz decomposition of the light-cone photon distribution amplitudes, the Wandzura-Wilczek–like relations associated with the transverse photon wave function are derived in a way similar to the rho meson, and the twist-two parts of the two photon wave functions, $h^{(s),\text{twist two}}_{\gamma\parallel}(u, P^2)$ and $h^{(t),\text{twist two}}_{\gamma\parallel}(u, P^2)$, are calculated besides the calculation of the leading-twist transverse photon wave functions with odd chirality, $\phi_{\gamma\perp}(u, P^2)$.

In this work, we re-examine both space-like and time-like off-shell (including on-shell) photon wave function corresponding to the chiral-odd operator with the Dirac matrix $\sigma_{\mu\nu}$, and study further all the possible off-shell chiral-odd photon wave functions which can be calculated from the leading-twist result. Unlike in our previous work [25], the parameter, Λ, which characterizes the pole formula for the instanton form factor $F(k)$, is determined not by imposing the normalization condition for the photon wave functions as done in ref. [26], but by the requirement that the value of Λ should be adjusted so that the pole form with definite integer n and this value of Λ reproduces well the theoretic form factor derived from the instanton model of QCD vacuum. The key observation for us to use this method to determine Λ is that the form factor $F(k)$ is, in fact, an intrinsic effective object in the low-energy theory, and should be independent of any hadron or photon wave functions.

In ref. [25], the integral appearing in the expressions of the transverse light-cone photon wave function, $\phi_{\gamma\perp}(u, P^2)$, and its coupling to the corresponding current, $f_{\gamma\perp}(P^2)$, is carried out over the whole momentum region from zero to infinity, but the momentum squared P^2 higher than some value lies out of the validity range of the low-energy effective theory. We note here that the so-called low energy in the low-energy effective theory is in fact related to the momentum squared P^2 according to the Lorentz invariance of the action in the dynamical theory, this means that only the transverse momentum squared in the light-cone frame should be confined in the low-energy region. To be consistent with the underlying effective dynamics, we should perform the integration for the transverse momentum over the finite range from zero to some upper bound $T(T^2 = v\Lambda^2)$, and let the dependence of the correlation function on this upper bound T (above T) be governed by the Brodsky-Lepage evolution equation which can be calculated in perturbative QCD [27]; while the wave function at a certain low-energy scale provides a necessary non-perturbative input for a complete QCD investigation. Furthermore, in the case of the longitudinal photon light-cone wave function [28], the similar integral turns out to be ultraviolet logarithmic divergent if the transverse momentum of the quark or the antiquark is unbounded, and if the form factor $F(k)$ serves to be the only ultraviolet cutoff. This logarithmic divergent integral for the transverse momentum should be dropped in the low-energy effective theory of QCD, and may be regularized by introducing a usual cutoff T. The same kind of integrals calculated from the same underlying effective theory should be treated at the same footing. This idea encourages us to use the latter as a unified way to deal with such integrals in the low-energy theory regardless of the integral being ultraviolet convergent or divergent.

Moreover, we have found that the choice of T for T being greater than some value has no significant influence on both the shapes and the values of the transverse photon wave function, because such kind of influences contributes, in a similar way, to both the numerator and the denominator of the r.h.s. of the resultant expression, eq. (22)

(see below), for the transverse photon wave function, and then strongly cancels. This key observation stimulates us to assume that the physical wave function is independent of this artificially introduced upper bound as it should be. Proceeding in this way, we have found that the above assumption can be realized provided the values of the cutoff T or v belong to the allowed regions. In the same spirit, we may demand that the physical coupling constant, $f_\gamma^\perp(P^2)$, should be independent of the artificial values of n. This constraint may be used to fix the possible value of T for definite n. In fact, such possible values of (n, T) really exist within the above allowed regions. We note here that with these obtained values of the cutoff T for different n, not only the coupling $f_\gamma^\perp(P^2)$ remains to be unchanged, but also the wave functions $\phi_{\gamma\perp}(u, P^2)$, $h_{\gamma\|}^{(s)}(u, P^2)$ and $h_{\gamma\|}^{(t)}(u, P^2)$ are less affected by a change of n.

The paper is organized as follows: We describe the definitions of the light-cone photon wave functions which are needed in our calculation with all notations being given in [25] in sect. 2. In sect. 3, two sum rules for calculating $\phi_{\gamma\perp}(u, P^2)$ within the low-energy effective theory of QCD, and the coupling constant, $f_\gamma^\perp(P^2)$, of the non-local quark-antiquark tensor current to the photon are derived. Before the numerical calculation, the values for (n, Λ) are determined from the requirement that both the physical wave function and its coupling to the corresponding current are insensitive to the choice of (n, Λ). Section 5 is devoted to the numerical simulation of $\phi_{\gamma\perp}(u, P^2)$ and its coupling $f_\gamma^\perp(P^2)$. In addition, the twist-two parts of the other two light-cone photon wave functions, $h_{\gamma\|}^{(s),\text{twist two}}(u, P^2)$ and $h_{\gamma\|}^{(t),\text{twist two}}(u, P^2)$ with odd chirality are calculated based on the Wandzura-Wilczek–like relations as well. Finally, the conclusions are given, and the behavior of the resultant photon wave functions and the coupling constant, $f_\gamma^\perp(P^2)$, are discussed. Moreover, to be clearer, a verification of the validity of the Wandzura-Wilczek–like relations in the photon case is presented as an appendix.

2 Definition of the chirality-violating photon wave functions

Now turn to the light-cone photon distribution amplitude. With the light-cone kinematics and notations described in ref. [23], the matrix element between the one-photon state and the vacuum is extracted from the correlation function of the light-ray operator with the electromagnetic current. As stated in ref. [25], the on- and off-shell light-cone photon distribution amplitude, namely the matrix element of a gauge invariant and the flavor-singlet quark-antiquark non-local operator between the vacuum and the one-photon state [29], can be expressed as

$$\begin{aligned}&\langle 0|\bar\psi(z)\Gamma[z,-z]\psi(-z)|\gamma(P,\lambda)\rangle \equiv\\ &i\int \mathrm{d}^4x e_\nu^{(\lambda)} e^{-iP\cdot x}\\ &\times\langle 0|T\big\{\bar\psi(z)\Gamma[z,-z]\psi(-z)j_{\text{em}}^\nu(x)\big\}|0\rangle,\end{aligned}\tag{1}$$

where a photon state is characterized by the momentum, P, and the polarization vector $e_\nu^{(\lambda)}$, z is a light-like separation between the quark and antiquark locations, Γ a Dirac Γ-matrix, and $[x, y]$ a path-ordered gauge factor along the straight line connecting the points x and y:

$$\begin{aligned}[x,y] = P\exp\Big\{i\int_0^1 \mathrm{d}\tau (x-y)_\mu \big[g_s B^\mu(\tau x+(1-\tau)y)\\ +Q_\psi A^\mu(\tau x+(1-\tau)y)\big]\Big\}\end{aligned}\tag{2}$$

with B^μ and A^μ being the gluon and photon potentials respectively, and $j_{\text{em}}^\nu(x) = Q_\psi\bar\psi(x)\gamma^\nu\psi(x)$ is the local electromagnetic current with Q_ψ being the electric charge of the quark field $\psi(x)$. We note that the r.h.s. of eq. (1) is really the expression for the on-shell photon-to-vacuum transition amplitude, and it may naturally be extended to be the definition of the photon-to-vacuum transition amplitude for P being space-like or time-like, namely $P^2 \neq 0$. In the latter case, it is convenient to define the light-like momentum p in such a way that it coincides with P in the limit $P^2 \to 0$, and $z\cdot p \neq 0$.

The Lorentz decomposition for the on/off-shell photon distribution amplitudes can be carried out in a way similar to the case of the rho meson. We may read off the Lorentz decomposition of the on/off-shell photon distribution amplitudes from the corresponding ones of the rho meson with the difference in isospin components [23]. A systematic Lorentz decomposition of the on- and off-shell photon distribution amplitudes [25] up to twist four has verified this statement up to a tiny difference in defining the scalar coupling constant. For the chirality-violating distributions, we have

$$\begin{aligned}&\langle 0|\bar\psi(z)\sigma_{\mu\nu}[z,-z]\psi(-z)|\gamma(P,\lambda)\rangle =\\ &if_\gamma^\perp\big(P^2\big)\Big[\Big(e_{\perp\mu}^{(\lambda)}p_\nu - e_{\perp\nu}^{(\lambda)}p_\mu\Big)\int_0^1 \mathrm{d}u e^{i\xi p\cdot z}\phi_{\gamma\perp}\big(u,P^2\big)\\ &+\big(p_\mu z_\nu - p_\nu z_\mu\big)\frac{e^{(\lambda)}\cdot z}{(p\cdot z)^2}P^2\int_0^1 \mathrm{d}u e^{i\xi p\cdot z}h_{\gamma\|}^{(t)}\big(u,P^2\big)\\ &+\text{higher twists}\Big],\end{aligned}\tag{3}$$

for the quark-antiquark tensor current, and

$$\begin{aligned}&\langle 0|\bar\psi(z)[z,-z]\psi(-z)|\gamma(P,\lambda)\rangle =\\ &-i\left(f_\gamma^\perp\big(P^2\big) - 2f_\gamma\big(P^2\big)\frac{m_q}{\mu}\right)\\ &\times\big(e^{(\lambda)}\cdot z\big)P^2\int_0^1 \mathrm{d}u e^{i\xi p\cdot z}h_{\gamma\|}^{(s)}\big(u,P^2\big),\end{aligned}\tag{4}$$

for the quark-antiquark scalar one, where we have used the usual assumption that the two partons, the quark and the antiquark, carry the momentum uP and $(1-u)P$ respectively, and we use the shorthand notations $\xi = 2u-1$ and $\mu = \sqrt{|P^2|}$. The decay constants f_γ and $f_\gamma^\perp$ are defined in such a way that all wave functions are normalized according to $\int_0^1 \mathrm{d}u\phi_\gamma^i(u,P^2) = 1$. The wave functions $h_{\gamma\|}^{(t)}$

and $h_{\gamma\parallel}^{(s)}$ receive contributions of both leading twist two and non-leading twist three, and the twist-two contributions are related to the transverse wave function $\phi_{\gamma\perp}$ by Wandzura-Wilczek–like relations [30]

$$h_{\gamma\parallel}^{(t),\text{twist two}}(u,P^2) = (2u-1)\left[\int_0^u \mathrm{d}v \frac{\phi_{\gamma\perp}(v,P^2)}{1-v} - \int_u^1 \mathrm{d}v \frac{\phi_{\gamma\perp}(v,P^2)}{v}\right], \quad (5)$$

$$h_{\gamma\parallel}^{(s),\text{twist two}}(u,P^2) = 2\left[\bar{u}\int_0^u \mathrm{d}v \frac{\phi_{\gamma\perp}(v,P^2)}{1-v} + u\int_u^1 \mathrm{d}v \frac{\phi_{\gamma\perp}(v,P^2)}{v}\right]. \quad (6)$$

The detailed proof for this point is given in the appendix.

3 Sum rules for the transverse photon wave function and its coupling constant

Now, we focus on the transverse photon wave function at the leading twist, $\phi_{\gamma\perp}(u,P^2)$. Combining eq. (1) with eq. (3), we have

$$\begin{aligned} &i\int \mathrm{d}^4x e_\sigma^{(\lambda)}(P) e^{-iP\cdot x}\langle 0|T\{\bar{\psi}(z)\sigma_{\mu\rho}[z,-z]\psi(-z)j_{\text{em}}^\sigma(x)\}|0\rangle = \\ &if_\gamma^\perp(P^2)\left[\left(e_{\perp\mu}^{(\lambda)}p_\rho - e_{\perp\rho}^{(\lambda)}p_\mu\right)\int_0^1 \mathrm{d}u e^{i\xi p\cdot z}\phi_{\gamma\perp}(u,P^2)\right. \\ &+\left(p_\mu z_\rho - p_\rho z_\mu\right)\frac{e^{(\lambda)}\cdot z}{(p\cdot z)^2}P^2\int_0^1 \mathrm{d}u e^{i\xi p\cdot z}h_{\gamma\parallel}^{(t)}(u,P^2) \\ &\left.+\text{higher twists}\right], \end{aligned} \quad (7)$$

where the contributions coming from the wave functions of twist being higher than three have been ignored. Multiplying both sides of the above equation by the photon polarization vector $e_\nu^{(\lambda)*}$, and summing over the polarization indices λ, we have

$$\begin{aligned} &\Pi_{\nu\mu\rho}(P) \equiv \\ &-i\int \mathrm{d}^4x e^{-iP\cdot x}\langle 0|T\{\bar{\psi}(z)\sigma_{\mu\rho}[z,-z]\psi(-z)j_\nu^{\text{em}}(x)\}|0\rangle = \\ &-if_\gamma^\perp(P^2)Q_\psi\left\{\left[(g_{\nu\mu}p_\rho - g_{\nu\rho}p_\mu) + \frac{p_\mu z_\rho - p_\rho z_\mu}{p\cdot z}p_\nu\right]\right. \\ &\times\int_0^1 \mathrm{d}u e^{i\xi p\cdot z}\phi_{\gamma\perp}(u,P^2) \\ &-\frac{1}{p\cdot z}(p_\mu z_\rho - p_\rho z_\mu)\left(p_\nu - \frac{P^2}{2p\cdot z}z_\nu\right) \\ &\left.\times\int_0^1 \mathrm{d}u e^{i\xi p\cdot z}h_{\gamma\parallel}^{(t)}(u,P^2)\right\}, \end{aligned} \quad (8)$$

which is consistent with eq. (31) in [22] apart from the new Lorentz structure

$$\frac{p_\mu z_\rho - p_\rho z_\mu}{p\cdot z}p_\nu \quad (9)$$

arising from the non-vanishing virtuality P^2 and the new contribution due to the appearance of $h_{\gamma\parallel}^{(t)}(u,P^2)$, where, in deriving the result, the usual formula for the polarization summation

$$\sum_\lambda e_\mu^{(\lambda)*}(P)e_\nu^{(\lambda)}(P) = -g_{\mu\nu} + \frac{P_\mu P_\nu}{P^2} \quad (10)$$

is used. We note that the coupling is rescaled as itself multiplied by Q_ψ in order to get the flavor-independent coupling. Finally, eliminating the contribution of $h_{\gamma\parallel}^{(t)}(u,P^2)$ leads to

$$\begin{aligned} &z^\mu\Pi_{\nu\mu\rho}(P) - \frac{z_\rho}{p\cdot z}\Pi_\nu(P) = \\ &iQf_\gamma^\perp(P^2)\left[g_{\nu\rho}p\cdot z - \left(p_\nu z_\rho + p_\rho z_\nu\right)\right] \\ &\times\int_0^1 \mathrm{d}u e^{i\xi p\cdot z}\phi_{\gamma\perp}(u,P^2). \end{aligned} \quad (11)$$

On the other hand, we can work out the correlation functions, $\Pi_{\nu\mu\rho}(P)$, at the leading electromagnetic coupling within the effective theory derived from the instanton model of the QCD vacuum

$$\begin{aligned} \Pi_{\nu\mu\rho}(P) = iQN_c\int\frac{\mathrm{d}^4k}{(2\pi)^4}e^{-i(2k-p)\cdot z} \\ \times\text{tr}\{\gamma_\nu S_F(P-k)\sigma_{\mu\rho}S_F(-k)\}, \end{aligned} \quad (12)$$

where $S_F(k)$ is the quark propagator. Combining with eq. (11), we obtain

$$\begin{aligned} &\phi_{\gamma\perp}(u,P^2) = \frac{N_c}{f_\gamma^\perp(P^2)}\int\frac{\mathrm{d}^4k}{(2\pi)^4}\delta(k^+ - up^+) \\ &\times\text{tr}\left\{\gamma^\nu S_F(P-k)\left(n^\mu\sigma_{\mu\nu} - \frac{n_\nu n^\mu}{p\cdot n}p^\sigma\sigma_{\mu\sigma}\right)S_F(-k)\right\}, \end{aligned} \quad (13)$$

where, for the sake of convenience, we have introduced n as dimensionless light-like vector parallel to z, with $z_\mu = n_\mu\tau$.

To evaluate the trace of the r.h.s. of eq. (13), we need the expression of the quark propagator of the low-energy effective theory of QCD. The instanton model of the QCD vacuum in the large-N_c limit predicts that quarks interact non-locally with an external meson field U through the following low-energy effective action [16,31]:

$$S_{\text{eff}} = -N_c\,\text{Tr}\ln(i\not{\partial} + iMFU^{\gamma_5}F), \quad (14)$$

where

$$U^{\gamma_5}(x) = \exp(i\gamma_5\tau^a\pi^a(x)). \quad (15)$$

M is the dynamical quark mass at zero momentum, which appears due to the spontaneous breaking of the chiral symmetry, and

$$M \approx 350\,\text{MeV} \quad (16)$$

and $F(k)$ is the form factor, related to the Fourier transform of the instanton zero mode [16]:

$$F(k) = 2y[I_0(y)K_1(y) - I_1(y)K_0(y)] - 2I_1(y)K_1(y) \quad (17)$$

with $y = k\rho/2$ with $1/\rho \sim 600\,\mathrm{MeV}$ being the typical inverse instanton size. Note that

$$F(k=0) = 1 \tag{18}$$

and the asymptotic behavior of the form factor is

$$F(k) \to 6/\big(k^3\rho^3\big), \qquad \text{for } -k^2 \gg \bar{\rho}^{-2}. \tag{19}$$

The leading-order quark propagator, $S_F(k)$, in the effective theory eq. (14) with the effective quark mass $MF^2(k)$, can be explicitly expressed as follows:

$$\int \mathrm{d}^4(x-y)e^{ik\cdot(x-y)}\langle 0|T\big\{\psi_{im\alpha}(x)\bar{\psi}_{jm\beta}(y)\big\}|0\rangle = i\delta_{ij}\delta_{mn}\left(\frac{\not{k}+MF^2(k)}{k^2-M^2F^4(k)+i\epsilon}\right)_{\alpha\beta}, \tag{20}$$

where i, j are the color indices in the $SU_c(3)$ fundamental representation, m, n are the flavor indices, and α, β the spinor indices. Using eq. (20), a straightforward manipulation leads to

$$\phi_{\gamma\perp}\big(u,P^2\big) = \frac{8iN_cMp^+}{f_\gamma^\perp\big(P^2\big)} \times \int \frac{\mathrm{d}^4k}{(2\pi)^4}\delta\big(k^+-up^+\big)D(k)D(k-P) \times\big[(1-u)F^2(k)+uF^2(k-P)\big] \tag{21}$$

Next, we may rewrite eq. (21) as

$$\phi_{\gamma\perp}\big(u,P^2\big) = I\big(u,P^2\big)\Big/\int_0^1 \mathrm{d}\omega I\big(\omega,P^2\big) \tag{22}$$

in corporation with the wave function normalization, where

$$I\big(u,P^2\big) = iMp^+\int\frac{\mathrm{d}^4k}{(2\pi)^4}\delta\big(k^+-up^+\big)D(k)D(k-P) \times\big[(1-u)F^2(k)+uF^2(k-P)\big]. \tag{23}$$

From the normalization condition for $\phi_{\gamma\perp}(u,P^2)$, we have

$$f_\gamma^\perp\big(P^2\big) = 8N_c\int_0^1 \mathrm{d}uI\big(u,P^2\big). \tag{24}$$

Equations (22) and (24) serve to be the sum rules for the transverse light-cone wave function $\phi_{\gamma\perp}(u,P^2)$ and for its coupling constant $f_\gamma^\perp(P^2)$ to the corresponding non-local quark-antiquark tensor current.

4 Determination of Λ for definite n in a pole form of the instanton form factor

We recall that the form factor $F(k)$ is derived for Euclidean (*i.e.*, space-like) momenta. To include very high moments in order to restore the end-point behavior of the wave functions, we would like to perform a calculation within the effective action directly in the Minkowskian space. To this end, we shall choose a pole formula for the form factor

$$F(k) = \left(\frac{-\Lambda^2}{k^2-\Lambda^2+i\epsilon}\right)^n, \tag{25}$$

where k is the Minkowskian momentum. In refs. [26,25], the cutoff parameter Λ has to be chosen in a way such that the normalization condition of the photon wave functions is fulfilled. However, as stated before, the form factor $F(k)$ is, in fact, an intrinsic object in the low-energy effective theory, and should be independent of any hadron or photon wave functions. Therefore, a reasonable way to determine the value of Λ for different integer n is that the derivation of the model pole form (25) from the theoretical form factor (17) in the Euclidean region of the momentum should be minimal. Our resultant values of Λ obtained in this way are listed in table 1 for $n = 1, 2, 5$, the comparison between the model pole form and the form factor derived from the instanton model is displayed in fig. 1. The latter really shows a good agreement between two forms of the form factor for $n = 1, 2$, while there is a not so-good agreement appearing at some large Euclidean momenta for the case of $n = 5$ which is also used in our numerical simulation for the purpose of comparison.

Now turn back to the transverse photon wave function at the leading twist eq. (22). Introducing the scaled variables

$$\eta = \frac{P^+k^-}{\Lambda^2}, \qquad t = \frac{\big|k^\perp\big|^2}{\Lambda^2}, \qquad s = \frac{P^2}{\Lambda^2}, \tag{26}$$

Table 1. The corresponding Λ parameters in the pole formula (25) for the form factor derived from the low-energy effective theory with n ranging from 1 to 5.

n	1	2	3	4	5
Λ(MeV)	850	1420	1800	2100	2380

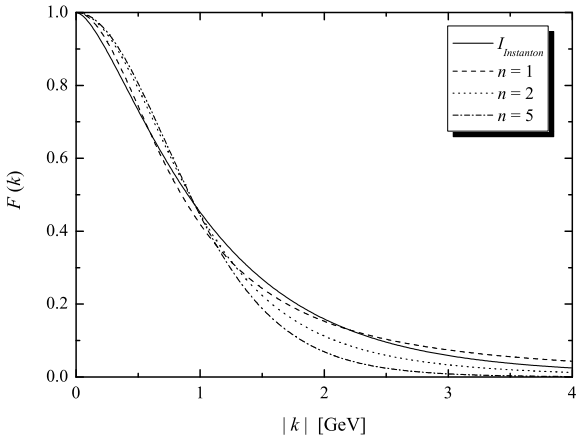

Fig. 1. The form factors $F(k)$ derived from the instanton vacuum model (solid line) as well as suggested with the pole forms (dashed line for $n = 1$, dotted line for $n = 2$ and dash-dotted line for $n = 5$).

after performing the integration over k^+ and over the azimuthal angle (taking the direction of the longitudinal momentum of the photon as the polar axis), we have

$$I(u,P^2)=\frac{iM}{4(2\pi)^3}\int \mathrm{d}t\int_{-\infty}^{+\infty}\mathrm{d}\eta\frac{(1-u)\xi_1^{2n}\xi_2^{4n}+u\xi_1^{4n}\xi_2^{2n}}{G(\xi_1)G(\xi_2)}\,, \tag{27}$$

where

$$\xi_1=u\eta-t-1+i\epsilon',\quad \xi_2=-(1-u)\eta-t-1+(1-u)s-i\epsilon'' \tag{28}$$

and

$$G(z)=z^{4n+1}+z^{4n}-\frac{M^2}{\Lambda^2}=\prod_{i=1}^{4n+1}(z-z_i); \tag{29}$$

z_i are roots of $G(z)=0$.

To ensure the wave function to be real, we choose the contour closing in the upper complex η half-plane so that all the zeros $\eta_i^{(2)}$ of $\xi_2(\eta)=0$ are enclosed in it, and none of the zeros $\eta_i^{(1)}$ of $\xi_1(\eta)=0$ are. We then complete the contour integration over η, and obtain

$$I\big(u,P^2\big)=\frac{M}{4(2\pi)^2}\int_0^v \mathrm{d}t\sum_{i,k}^{4n+1}f_if_k\Big[uz_k^{4n}z_i^{2n}+(1-u)z_k^{2n}z_i^{4n}\Big]\times\frac{1}{t+1+uz_i+(1-u)z_k-u(1-u)s}\,, \tag{30}$$

where f_i is defined as

$$f_i=\prod_{j=1,j\neq i}^{4n+1}\frac{1}{z_j-z_i}\,. \tag{31}$$

In accomplishing the integration over t, we have introduced an upper bound, $T^2=v\Lambda^2$, in a way as described in ref. [24]:

$$\phi\big(x,P^2\big)\sim\int_{k_\perp^2<T^2}\mathrm{d}^2k_\perp\phi\big(x,\mathbf{k}_\perp,P^2\big)$$

and the dependence of the wave function on the scale T (above T) is governed by the Brodsky-Lepage evolution equation [27], and can be calculated in perturbative QCD, while the wave function at a certain low-energy scale provides a necessary non-perturbative input for a complete QCD investigation. Therefore, at the regularization scale T or equivalently the dimensionless one v, we have

$$I\big(v,u,P^2\big)=\frac{M}{4(2\pi)^2}\sum_{i,k}^{4n+1}f_if_k\Big[uz_k^{4n}z_i^{2n}+\bar{u}z_k^{2n}z_i^{4n}\Big]\times\ln\left(1+\frac{v}{1+uz_i+\bar{u}z_k-u\bar{u}s}\right). \tag{32}$$

The arbitrary choice of the regularization scale T or v may bring some arbitrariness to our evaluation of the coupling constant as well as of the photon wave functions. An important observation is that the influence of the choice of the value of T on the wave function $\phi_{\gamma\perp}(u,P^2)$ is very weak, because such kind of influences contributes, in a similar way, to both the numerator and denominator of eq. (22), and thus strongly cancels. However, we have found that the choice of the value of T has significant effect on the determination of the coupling constant $f_\gamma^\perp(P^2)$. To take away this shortcoming, we should fix the regularization scale T or find a region of T, where the influence of T on the coupling becomes insensitive, from some physical ground. For this purpose, our key assumption is that the wave function $\phi_{\gamma\perp}(u,P^2)$ is, in fact, independent of the

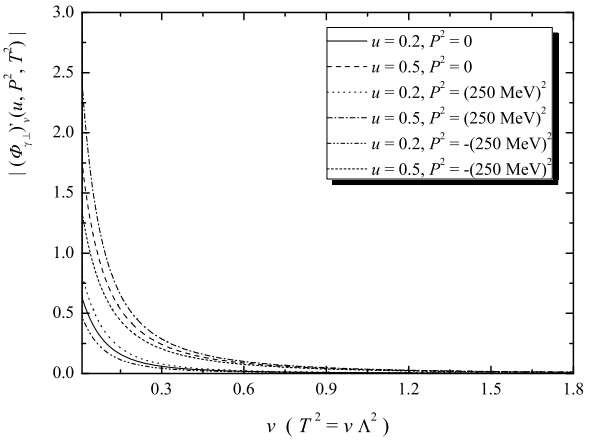

Fig. 2. The absolute value of the partial derivative on the transverse photon wave function, $|(\phi_{\gamma\perp})'_v(v,u,P^2)|$, with respect to v *versus* the value of v with $n=1$ and $M=350\,\mathrm{MeV}$ in the cases of $(u,P^2\,[\mathrm{MeV}^2])$ being $(0.2,0)$, $(0.5,0)$, $(0.2,250^2)$, $(0.5,250^2)$, $(0.2,-250^2)$ and $(0.5,-250^2)$.

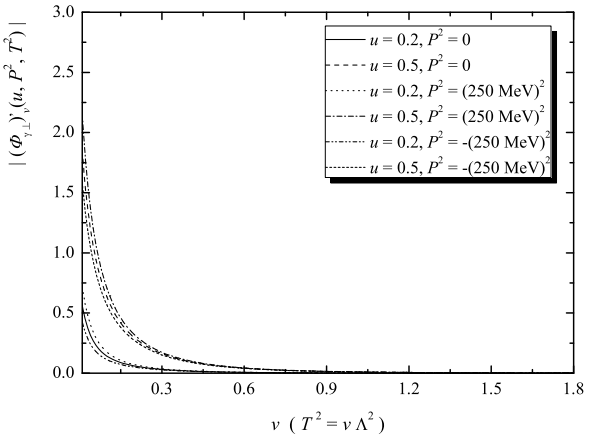

Fig. 3. The absolute value of the partial derivative on the transverse photon wave function, $|(\phi_{\gamma\perp})'_v(v,u,P^2)|$, with respect to v *versus* the value of v with $n=2$ and $M=350\,\mathrm{MeV}$ in the cases of $(u,P^2\,[\mathrm{MeV}^2])$ being $(0.2,0)$, $(0.5,0)$, $(0.2,250^2)$, $(0.5,250^2)$, $(0.2,-250^2)$ and $(0.5,-250^2)$.

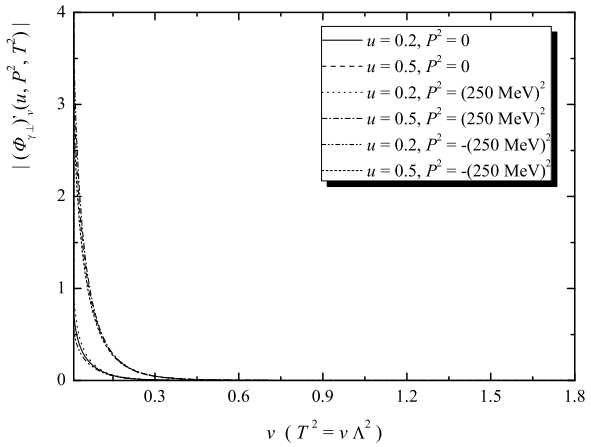

Fig. 4. The absolute value of the partial derivative on the transverse photon wave function, $|(\phi_{\gamma\perp})'_v(v,u,P^2)|$, with respect to v *versus* the value of v with $n = 5$ and $M = 350\,\mathrm{MeV}$ in the cases of $(u, P^2\ [\mathrm{MeV}^2])$ being $(0.2, 0)$, $(0.5, 0)$, $(0.2, 250^2)$, $(0.5, 250^2)$, $(0.2, -250^2)$ and $(0.5, -250^2)$.

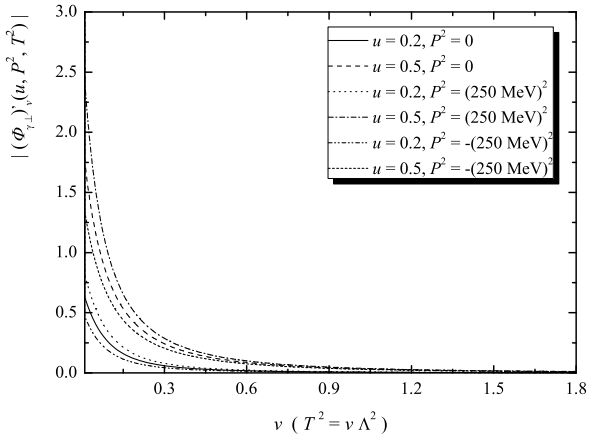

Fig. 5. The absolute value of the partial derivative on the transverse photon wave function, $|(\phi_{\gamma\perp})'_v(v,u,P^2)|$, with respect to v *versus* the value of v with $n = 1$ and $M = 400\,\mathrm{MeV}$ in the cases of $(u, P^2\ [\mathrm{MeV}^2])$ being $(0.2, 0)$, $(0.5, 0)$, $(0.2, 250^2)$, $(0.5, 250^2)$, $(0.2, -250^2)$ and $(0.5, -250^2)$.

artificial choice of T, and so is the r.h.s. of eq. (22), *i.e.*

$$\Delta(v,u,P^2) \equiv \int_0^1 \mathrm{d}\omega I'_v(v,u,P^2) I(v,\omega,P^2) - \int_0^1 \mathrm{d}\omega I(v,u,P^2) I'_v(v,\omega,P^2) = 0, \quad (33)$$

which may serve to be the condition to determine the value of the regularization scale T or of its allowed region. The condition (33) can be rewritten in a differential form

$$(\phi_{\gamma\perp})'_v(v,u,P^2) = \Delta(v,u,P^2) \Big/ \left[\int_0^1 \mathrm{d}\omega I(v,\omega,P^2)\right]^2 = 0 \quad (34)$$

The curves of $|(\phi_{\gamma\perp})'_v(v,u,P^2)|$ *versus* v for different values of u and P^2 are shown in figs. 2-7.

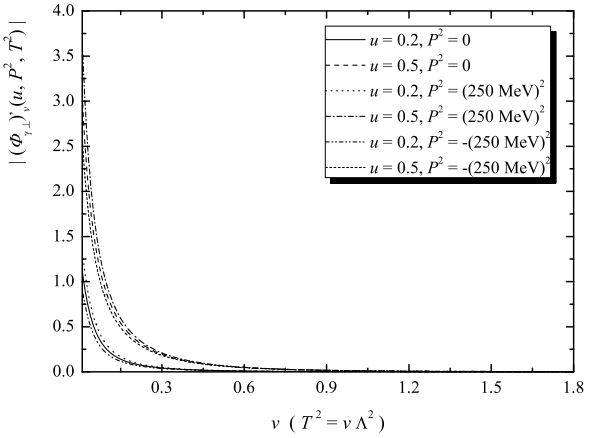

Fig. 6. The absolute value of the partial derivative on the transverse photon wave function, $|(\phi_{\gamma\perp})'_v(v,u,P^2)|$, with respect to v *versus* the value of v with $n = 2$ and $M = 400\,\mathrm{MeV}$ in the cases of $(u, P^2\ [\mathrm{MeV}^2])$ being $(0.2, 0)$, $(0.5, 0)$, $(0.2, 250^2)$, $(0.5, 250^2)$, $(0.2, -250^2)$ and $(0.5, -250^2)$.

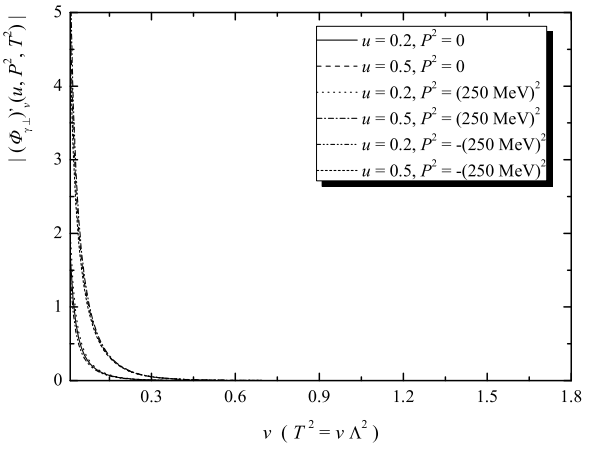

Fig. 7. The absolute value of the partial derivative on the transverse photon wave function, $|(\phi_{\gamma\perp})'_v(v,u,P^2)|$, with respect to v *versus* the value of v with $n = 5$ and $M = 400\,\mathrm{MeV}$ in the cases of $(u, P^2\ [\mathrm{MeV}^2])$ being $(0.2, 0)$, $(0.5, 0)$, $(0.2, 250^2)$, $(0.5, 250^2)$, $(0.2, -250^2)$ and $(0.5, -250^2)$.

In figs. 2-7, we can see that for the case of $n = 1$, $T \geq 1.1\,\mathrm{GeV}$, corresponding to $v \geq 1.6$, may be reasonably good enough to get a regularization scale independent wave function. Similarly, for the cases of $n = 2$ or 5, the good choice may be $v \geq 0.9$ (*i.e.* $T \geq 1.3\,\mathrm{GeV}$) or $v \geq 0.45$ (*i.e.* $T \geq 1.6\,\mathrm{GeV}$).

5 Numerical simulation

As an input in the numerical simulation, the color number N_c is taken to be the real value, three; the integer, n, which characterizes the form factor, $F(k)$, described in the pole formulae eq. (25), is chosen to be 1, 2 or 5; and the mass parameter, M, which appears as the mass scale in the momentum-dependent quark mass, $M(k) = MF^2(k)$, is put to be 350 MeV or 400 MeV.

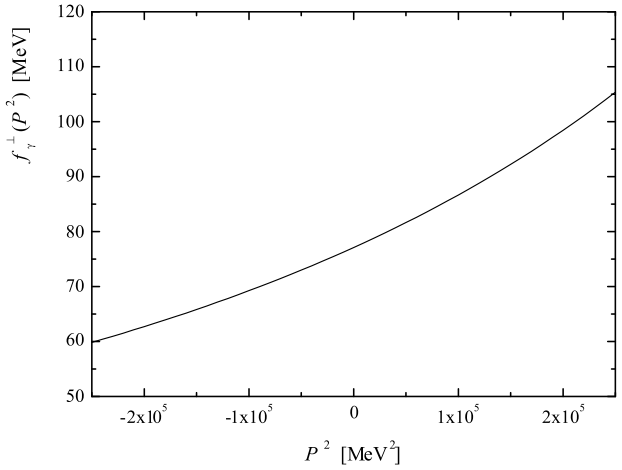

Fig. 8. The coupling $f_\gamma^\perp(P^2)$ for the case of $M = 350\,\mathrm{MeV}$.

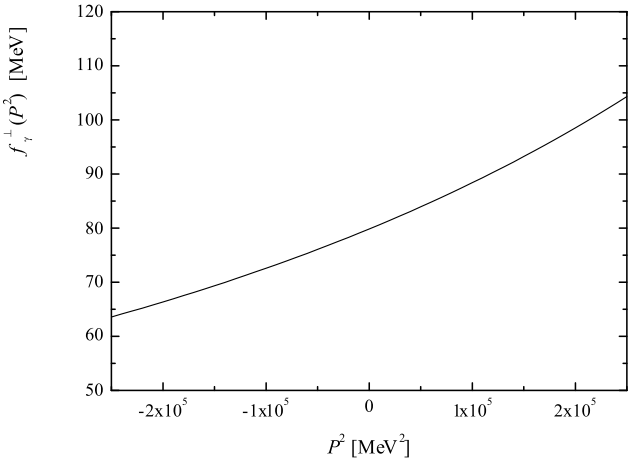

Fig. 9. The coupling $f_\gamma^\perp(P^2)$ for the case of $M = 400\,\mathrm{MeV}$.

Table 2. The parameters $f_\gamma^\perp(0)$ and a of the pole form of the coupling constant $f_\gamma^\perp(P^2)$ for different effective mass.

M [MeV]	$f_\gamma^\perp(0)$	a	M [MeV]	$f_\gamma^\perp(0)$	a
350	77.1	2.54	400	79.8	2.89

For the choice of $n = 1$, the value of Λ is taken to be $\Lambda^2 = 2.0\bar{\rho}^{-2} \simeq 2.0 \times 600^2\,\mathrm{MeV}^2$. The upper bound of the transverse momentum squared, T, for the integral $I(u, P^2)$ (or more explicitly $I(v, u, P^2)$), is chosen to be $1.2\,\mathrm{GeV}$ (*i.e.*, $v = 1.9$) according to our investigation above. The corresponding coupling constant $f_\gamma^\perp(P^2)$ for different choices in effective quark mass, $M = 350$ and $400\,\mathrm{MeV}$, is then determined by eq. (24), and displayed in fig. 8 and fig. 9, respectively. In addition, we have found that the coupling constant for momenta in the range $-(500\,\mathrm{MeV})^2 < P^2 < (500\,\mathrm{MeV})^2$ can be well cased in the pole form

$$f_\gamma^\perp(P^2) \simeq f_\gamma^\perp(0)\left(1 - \frac{P^2}{a\,\bar{\rho}^{-2}}\right)^{-1} \qquad (35)$$

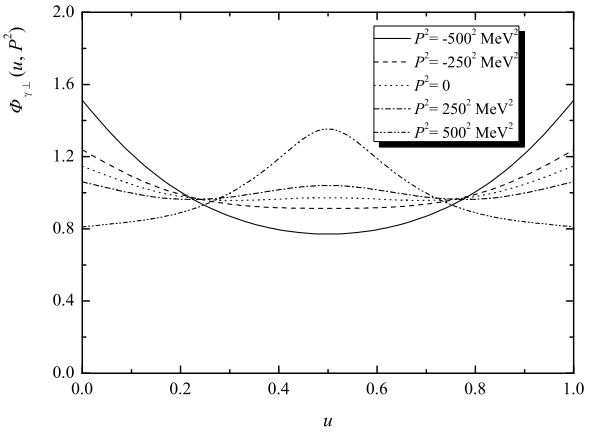

Fig. 10. The photon wave function, $\phi_{\gamma\perp}(u, P^2)$, for the case of $M = 350\,\mathrm{MeV}$, $n = 1$.

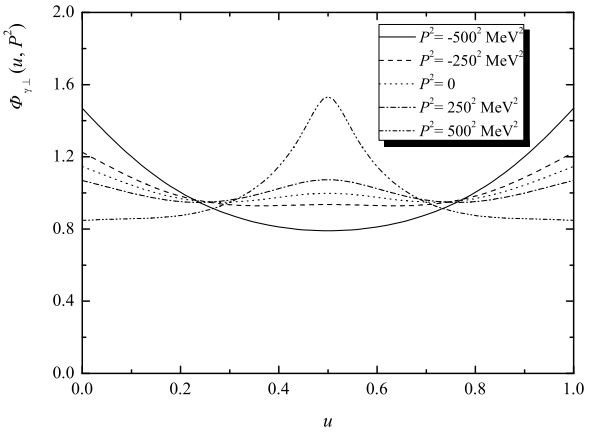

Fig. 11. The photon wave function, $\phi_{\gamma\perp}(u, P^2)$, for the case of $M = 400\,\mathrm{MeV}$, $n = 1$.

with $f_\gamma^\perp(0)$ and a being listed in table 2 for $M = 350\,\mathrm{MeV}$ or $400\,\mathrm{MeV}$, respectively.

For cases of $n > 1$, it is necessary to point out that $f_\gamma^\perp(P^2)$ should be, in fact, independent of n, because n is artificially introduced from the pole formula, eq. (25), for the form factor. This consideration can be used to fix the suitable values of the cutoff T (or v) for different $n > 1$. Our results are

$$T = 1.3\,\mathrm{GeV},\ \text{or equivalently}\ v = 0.9,\ \text{for}\ n = 2,$$
$$T = 1.6\,\mathrm{GeV},\ \text{or equivalently}\ v = 0.45,\ \text{for}\ n = 5.$$

According to eqs. (22), (23), the corresponding curves of $\phi_{\gamma\perp}(u, P^2)$ *versus* u with $n = 1$ or 2 or 5 and $M = 350\,\mathrm{MeV}$ or $M = 400\,\mathrm{MeV}$ are displayed in figs. 10-15, where the solid lines correspond to the case of $P^2 = -(500\,\mathrm{MeV})^2$, the dashed lines to the case of $P^2 = -(250\,\mathrm{MeV})^2$, the dotted line to $P^2 = 0$, the dash-dotted line to $P^2 = (250\,\mathrm{MeV})^2$, and the dash–double-dotted line to $P^2 = (500\,\mathrm{MeV})^2$.

Substituting eq. (22) into the Wandzura-Wilczek–like relations, eqs. (5) and (6), the twist-two parts of the wave

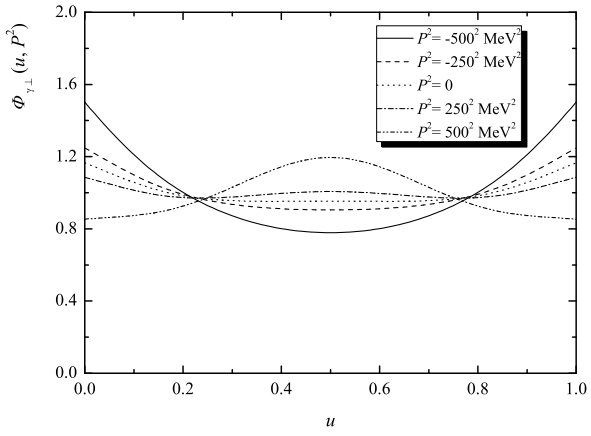

Fig. 12. The photon wave function, $\phi_{\gamma\perp}(u, P^2)$, for the case of $M = 350\,\mathrm{MeV}$, $n = 2$.

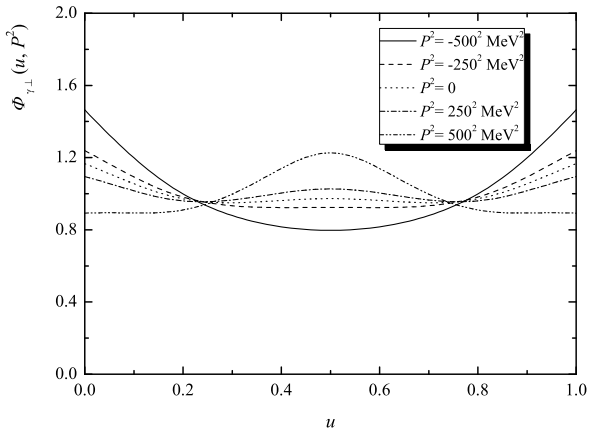

Fig. 13. The photon wave function, $\phi_{\gamma\perp}(u, P^2)$, for the case of $M = 400\,\mathrm{MeV}$, $n = 2$.

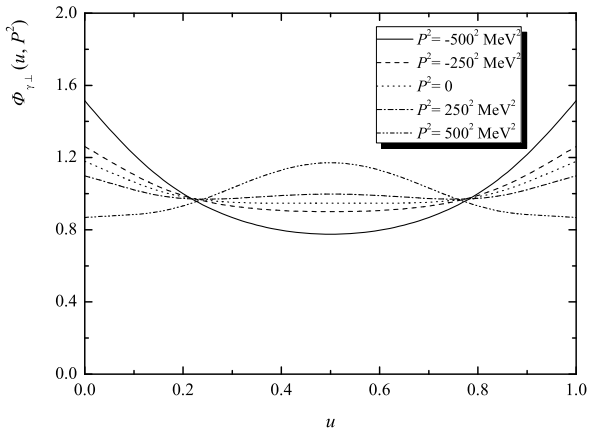

Fig. 14. The photon wave function, $\phi_{\gamma\perp}(u, P^2)$, for the case of $M = 350\,\mathrm{MeV}$, $n = 5$.

functions, $h_{\gamma\|}^{(s),\text{twist two}}$ and $h_{\gamma\|}^{(t),\text{twist two}}$, have been calculated, and displayed in figs. 16-27.

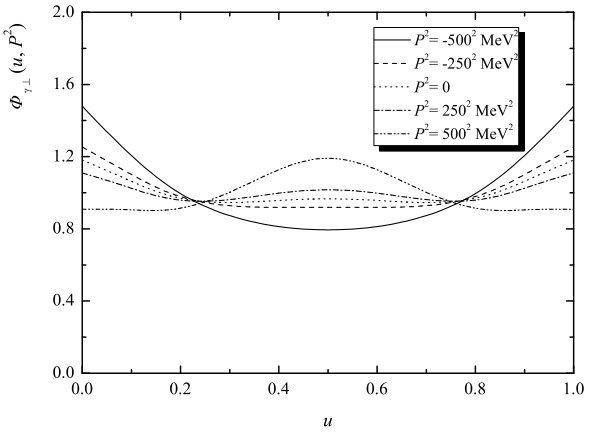

Fig. 15. The photon wave function, $\phi_{\gamma\perp}(u, P^2)$, for the case of $M = 400\,\mathrm{MeV}$, $n = 5$.

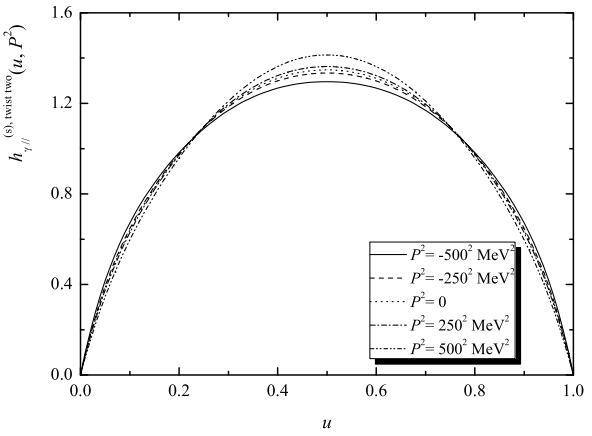

Fig. 16. The photon wave function, $h_{\gamma\|}^{(s),\text{twist two}}$, for the case of $M = 350\,\mathrm{MeV}$, $n = 1$.

6 Conclusion and discussion

In summary, we have computed the on-shell and off-shell photon wave functions with odd chirality at the leading twist in the effective low-energy theory derived from the instanton vacuum. We note here that besides the original Lorentz structure given in ref. [22], a new Lorentz structure (9) is found in the equivalent definition of the photon wave functions given in eq. (8). However, it turns out that this new term has no contribution to $\phi_\gamma^\perp(u, P^2)$. We also note here that the momentum of the virtual photon is not confined in the space-like region as in ref. [22], the time-like region of the momentum is considered too. We have worked out the explicit expression of the transverse photon wave function, $\phi_\gamma^\perp(u, P^2)$, at the leading twist. Then, the twist-two parts of the other two photon wave functions, $h_{\gamma\|}^{(s),\text{twist two}}(u, P^2)$ and $h_{\gamma\|}^{(t),\text{twist two}}(u, P^2)$, are calculated based on the Wandzura-Wilczek–like relations, eqs. (5) and (6).

For the numerical simulation, the only input parameters are adopted from the parameters of that effective low-energy theory. Therefore, the reliability of the calculated wave functions is related to approximations made in

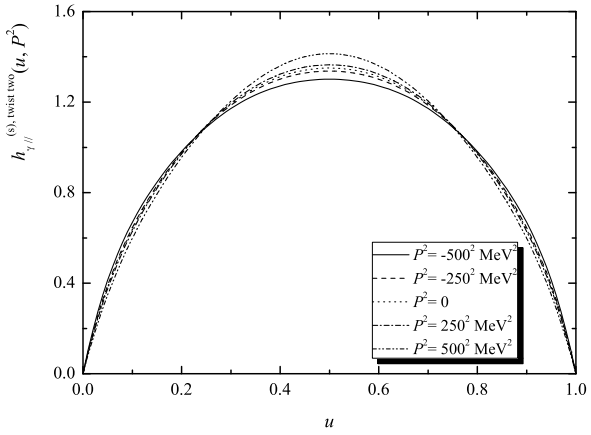

Fig. 17. The photon wave function, $h_{\gamma\|}^{(s),\text{twist two}}$, for the case of $M = 400\,\text{MeV}$, $n = 1$.

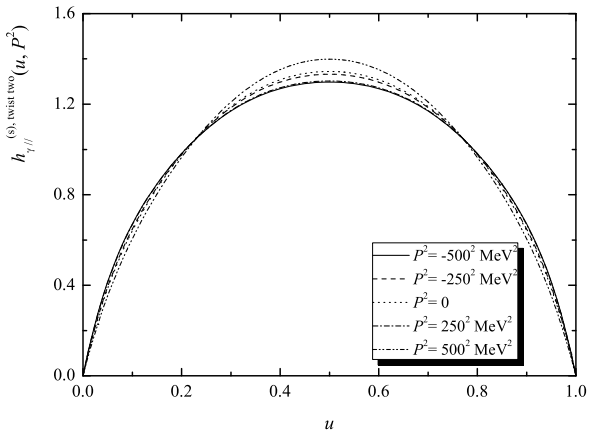

Fig. 18. The photon wave function, $h_{\gamma\|}^{(s),\text{twist two}}$, for the case of $M = 350\,\text{MeV}$, $n = 2$.

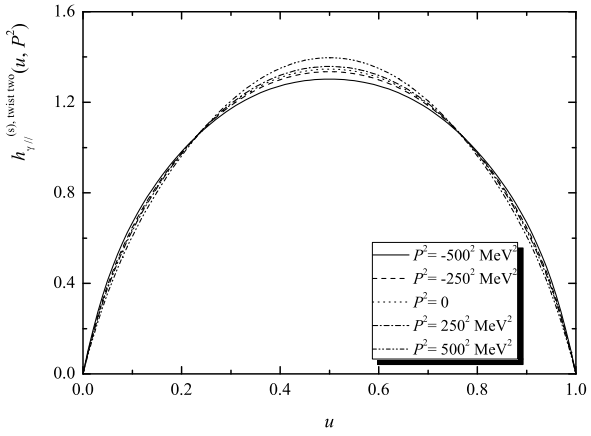

Fig. 19. The photon wave function, $h_{\gamma\|}^{(s),\text{twist two}}$, for the case of $M = 400\,\text{MeV}$, $n = 2$.

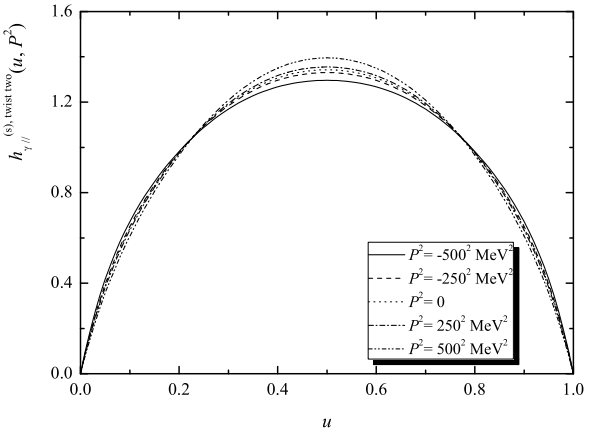

Fig. 20. The photon wave function, $h_{\gamma\|}^{(s),\text{twist two}}$, for the case of $M = 350\,\text{MeV}$, $n = 5$.

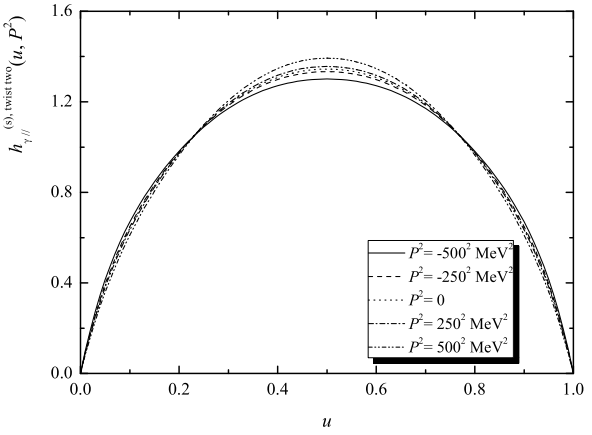

Fig. 21. The photon wave function, $h_{\gamma\|}^{(s),\text{twist two}}$, for the case of $M = 400\,\text{MeV}$, $n = 5$.

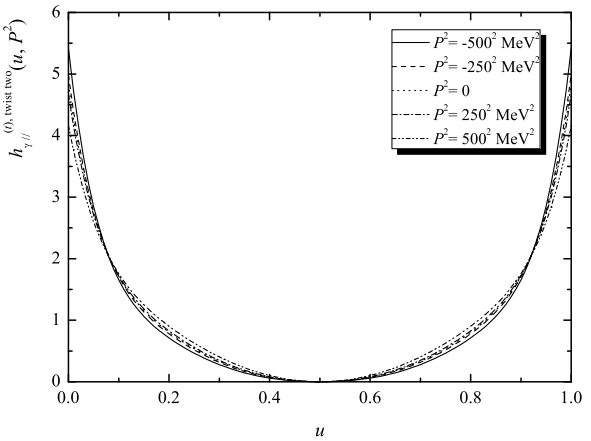

Fig. 22. The photon wave function, $h_{\gamma\|}^{(t),\text{twist two}}$, for the case of $M = 350\,\text{MeV}$, $n = 1$.

the instanton model of the QCD vacuum, which is based on the diluteness of the instantons in the vacuum, namely the smallness of the packing fraction $\bar{\rho}/\bar{R} = 1/3$. However, our qualitative predictions for the different behavior of the different photon wave functions with odd chirality are unambiguous at least to the leading order in $\bar{\rho}/\bar{R}$.

From figs. 8 and 9, we see that the value of the coupling, $f_\gamma^\perp(P^2)$, increases with P^2. From figs. 10-27, we can

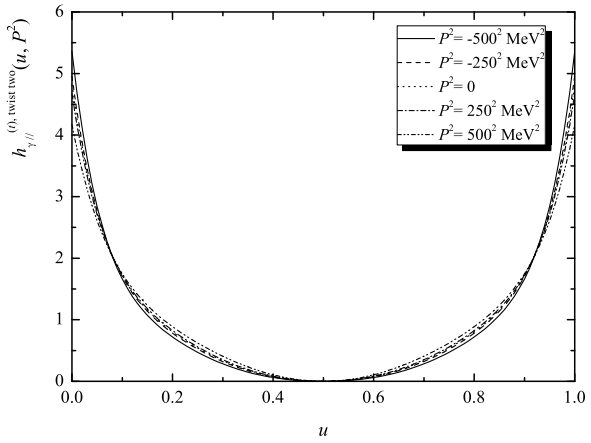

Fig. 23. The photon wave function, $h_{\gamma\|}^{(t),\text{twist two}}$, for the case of $M = 400\,\text{MeV}$, $n = 1$.

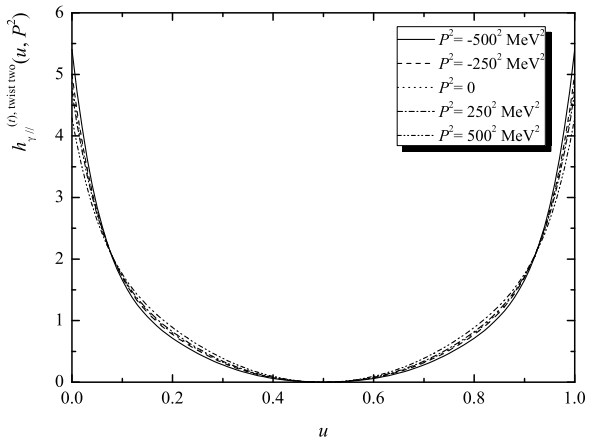

Fig. 24. The photon wave function, $h_{\gamma\|}^{(t),\text{twist two}}$, for the case of $M = 350\,\text{MeV}$, $n = 2$.

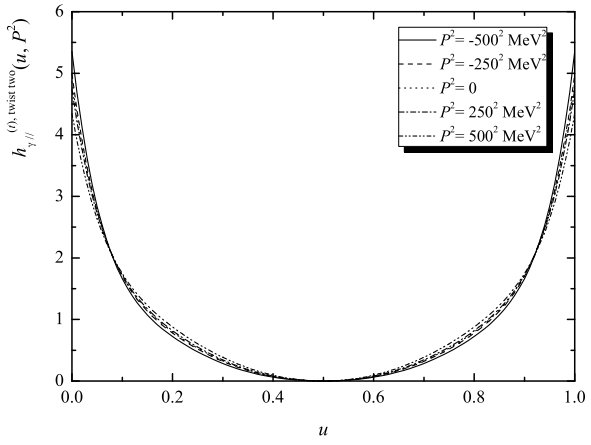

Fig. 25. The photon wave function, $h_{\gamma\|}^{(t),\text{twist two}}$, for the case of $M = 400\,\text{MeV}$, $n = 2$.

see that the photon wave function, $\phi_{\gamma\perp}(u, P^2)$, varies apparently with the variation of P^2 from $-(500\,\text{MeV})^2$ to $(500\,\text{MeV})^2$, while the twist-two part of the photon wave function, $h_{\gamma\|}^{(s),\text{twist two}}(u, P^2)$, varies less apparently, and

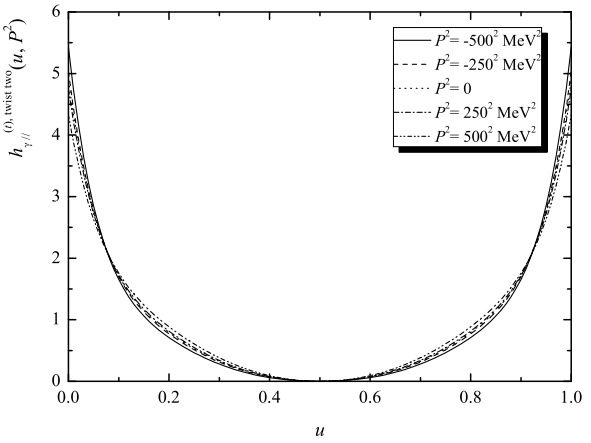

Fig. 26. The photon wave function, $h_{\gamma\|}^{(t),\text{twist two}}$, for the case of $M = 350\,\text{MeV}$, $n = 5$.

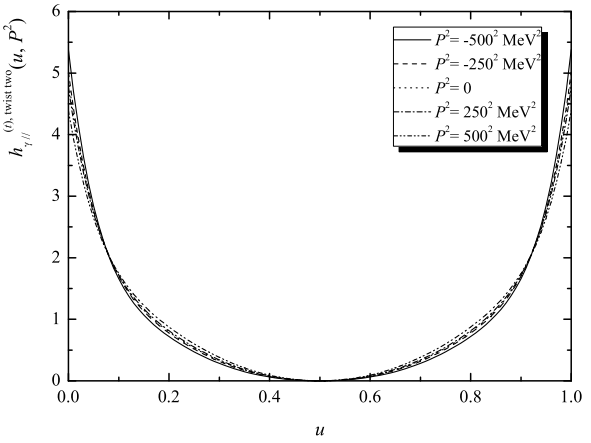

Fig. 27. The photon wave function, $h_{\gamma\|}^{(t),\text{twist two}}$, for the case of $M = 400\,\text{MeV}$, $n = 5$.

$h_{\gamma\|}^{(t),\text{twist two}}(u, P^2)$, varies very little. All displayed photon wave functions are symmetric with the transformation $u \to 1 - u$; this is obviously due to the fact that the currents associated with the corresponding photon wave functions are symmetric under the exchange between the quark and the antiquark fields.

Now, turn to the end-point behavior of the calculated photon wave functions. From the curves of the photon wave functions, we can see that

$$\phi_{\gamma\perp}\big(0, P^2\big) = \phi_{\gamma\perp}\big(1, P^2\big) \neq 0, \tag{36}$$

$$h_{\gamma\|}^{(t),\text{twist two}}\big(0, P^2\big) = h_{\gamma\|}^{(t),\text{twist two}}\big(1, P^2\big) \neq 0, \tag{37}$$

$$h_{\gamma\|}^{(s),\text{twist two}}\big(0, P^2\big) = h_{\gamma\|}^{(s),\text{twist two}}\big(1, P^2\big) = 0. \tag{38}$$

The end-point behavior of the photon wave function $h_{\gamma\|}^{(s),\text{twist two}}(u, P^2)$, *i.e.* eq. (38), is natural, and the reason for that behavior can be easily traced back to the Wandzura-Wilczek–like relation, eq. (6), according to which eq. (38) is valid because of the finiteness of $\phi_{\gamma\perp}(0, P^2) = \phi_{\gamma\perp}(1, P^2)$ and of the pre-factors u or $1 - u$ for the corresponding integrations. It is also obvious

Table 3. Gegenbauer coefficients of $\phi_{\gamma\perp}(u, P^2)$ with $n = 1$ and $M = 350\,\mathrm{MeV}$.

P^2 [MeV^2]	A	a_0	a_2	a_4	a_6
-500^2	1.51298	−0.51298	−0.01138	0.00114	0.00036
-250^2	1.23719	−0.23719	−0.01027	0.00305	−0.00005
0	1.14836	−0.14836	−0.01421	0.00444	−0.00054
250^2	1.06192	−0.06194	−0.02077	0.00645	−0.00159
500^2	0.83034	0.16942	−0.06374	0.01727	−0.01420

Table 4. Gegenbauer coefficients of $\phi_{\gamma\perp}(u, P^2)$ with $n = 1$ and $M = 400\,\mathrm{MeV}$.

P^2 [MeV^2]	A	a_0	a_2	a_4	a_6
-500^2	1.46901	−0.46900	−0.00879	0.00223	0.00034
-250^2	1.22532	−0.22532	−0.01314	0.00524	−0.00096
0	1.14816	−0.14818	−0.01874	0.00717	−0.00232
250^2	1.07430	−0.07436	−0.02716	0.00970	−0.00474
500^2	0.89692	0.10249	−0.08299	0.01974	−0.03023

Table 5. Gegenbauer coefficients of $\phi_{\gamma\perp}(u, P^2)$ with $n = 2$ and $M = 350\,\mathrm{MeV}$.

P^2 [MeV^2]	A	a_0	a_2	a_4	a_6
-500^2	1.50182	−0.50182	−0.01147	0.00188	0.00050
-250^2	1.24754	−0.24753	−0.00946	0.00317	0.00045
0	1.16525	−0.16524	−0.11802	0.00391	0.00035
250^2	1.08448	−0.08448	−0.01579	0.00491	0.00015
500^2	0.85405	0.14594	−0.03861	0.01035	−0.00171

Table 6. Gegenbauer coefficients of $\phi_{\gamma\perp}(u, P^2)$ with $n = 2$ and $M = 400\,\mathrm{MeV}$.

P^2 [MeV^2]	A	a_0	a_2	a_4	a_6
-500^2	1.46339	−0.46338	−0.00926	0.00352	0.00050
-250^2	1.23774	−0.23773	−0.01176	0.00578	−0.00004
0	1.16550	−0.16549	−0.01523	0.00702	−0.00050
250^2	1.09511	−0.09510	−0.02017	0.00859	−0.00122
500^2	0.89872	0.10121	−0.04553	0.01577	−0.00651

Table 7. Gegenbauer coefficients of $\phi_{\gamma\perp}(u, P^2)$ with $n = 5$ and $M = 350\,\mathrm{MeV}$.

P^2 [MeV^2]	A	a_0	a_2	a_4	a_6
-500^2	1.51425	−0.51424	−0.01161	0.00286	0.00056
-250^2	1.26006	−0.26004	−0.00936	0.00398	0.00060
0	1.17802	−0.17801	−0.01136	0.00454	0.00057
250^2	1.09754	−0.09752	−0.01483	0.00529	0.00050
500^2	0.86708	0.13294	−0.03463	0.00928	−0.00026

Table 8. Gegenbauer coefficients of $\phi_{\gamma\perp}(u, P^2)$ with $n = 5$ and $M = 400\,\mathrm{MeV}$.

P^2 [MeV^2]	A	a_0	a_2	a_4	a_6
-500^2	1.47756	−0.44753	−0.00940	0.00507	0.00052
-250^2	1.25123	−0.25120	−0.01151	0.00719	0.00017
0	1.17888	−0.17886	−0.01455	0.00826	−0.00010
250^2	1.10833	−0.10831	−0.01882	0.00958	−0.00053
500^2	0.90949	−0.09051	−0.03975	0.01542	−0.00336

Table 9. Gegenbauer coefficients of $h_{\gamma\|}^{(s),\text{twist two}}(u,P^2)$ with $n=1$ and $M=350\,\text{MeV}$.

P^2 [MeV^2]	b_2	b_4	b_6
-500^2	0.08271	0.01633	0.00358
-250^2	0.06748	0.01350	0.00292
0	0.06190	0.01263	0.00269
250^2	0.05592	0.01184	0.00245
500^2	0.03581	0.01007	0.00145

Table 10. Gegenbauer coefficients of $h_{\gamma\|}^{(s),\text{twist two}}(u,P^2)$ with $n=1$ and $M=400\,\text{MeV}$.

P^2 [MeV^2]	b_2	b_4	b_6
-500^2	0.08069	0.01593	0.00348
-250^2	0.06633	0.01351	0.00286
0	0.06108	0.01281	0.00263
250^2	0.05555	0.01219	0.00237
500^2	0.03633	0.01095	0.00104

Table 11. Gegenbauer coefficients of $h_{\gamma\|}^{(s),\text{twist two}}(u,P^2)$ with $n=2$ and $M=350\,\text{MeV}$.

P^2 [MeV^2]	b_2	b_4	b_6
-500^2	0.08208	0.01626	0.00356
-250^2	0.06819	0.01361	0.00296
0	0.06320	0.01278	0.00276
250^2	0.05802	0.01198	0.00256
500^2	0.04133	0.00987	0.00195

Table 12. Gegenbauer coefficients of $h_{\gamma\|}^{(s),\text{twist two}}(u,P^2)$ with $n=2$ and $M=400\,\text{MeV}$.

P^2 [MeV^2]	b_2	b_4	b_6
-500^2	0.08029	0.01560	0.00347
-250^2	0.06726	0.01368	0.00292
0	0.06264	0.01299	0.00273
250^2	0.05788	0.01234	0.00254
500^2	0.04267	0.01071	0.00189

Table 13. Gegenbauer coefficients of $h_{\gamma\|}^{(s),\text{twist two}}(u,P^2)$ with $n=5$ and $M=350\,\text{MeV}$.

P^2 [MeV^2]	b_2	b_4	b_6
-500^2	0.08275	0.01646	0.00359
-250^2	0.06891	0.01380	0.00299
0	0.06399	0.01296	0.00280
250^2	0.05891	0.01214	0.00261
500^2	0.04272	0.00993	0.00204

Table 14. Gegenbauer coefficients of $h_{\gamma\|}^{(s),\text{twist two}}(u,P^2)$ with $n=5$ and $M=400\,\text{MeV}$.

P^2 [MeV^2]	b_2	b_4	b_6
-500^2	0.08106	0.01621	0.00351
-250^2	0.06806	0.01392	0.00296
0	0.06350	0.01322	0.00278
250^2	0.05884	0.01255	0.00260
500^2	0.04424	0.01080	0.00203

that such pre-factors are absent for the Wandzura-Wilczek–like relation, eq. (5), of the photon wave function $h_{\gamma\|}^{(t),\text{twist two}}(u,P^2)$, and it is thus naturally to expect that both wave functions $\phi_{\gamma\perp}(u,P^2)$ and $h_{\gamma\|}^{(t),\text{twist two}}(u,P^2)$ would have the same end-point behavior. It is noticed that there is a common pre-factor, $2u-1$, in the r.h.s. of the same Wandzura-Wilczek–like relation, eq. (5), of the photon wave function $h_{\gamma\|}^{(t),\text{twist two}}(u,P^2)$; this directly leads to the observed middle-point behavior of the wave function $h_{\gamma\|}^{(t),\text{twist two}}(u,P^2)$, namely

$$h_{\gamma\|}^{(t),\text{twist two}}\big(u=1/2,P^2\big)=0. \tag{39}$$

As for the end-point behavior of the wave function $\phi_{\gamma\perp}(u,P^2)$, what we have obtained is in contradiction with the sum rule result in ref. [6] (namely, not in favor of the asymptotic form when the energy scale is low, and far from the asymptotic region of QCD), but is the same as that in refs. [22,25] for the light-like or space-like momentum, and similar for the time-like momentum. Here the word "similar" means that the end-point value of $\phi_{\gamma\perp}(u,P^2)$ is not only non-zero but also lower than that in the cases of the light-like or space-like momentum. The reason for the non-vanishing end-point value of $\phi_{\gamma\perp}(u,P^2)$ is that the photon-quark coupling is local while the pion-quark coupling is non-local as shown in the effective low-energy theory that we adopted to calculate the wave functions, and thus the form factor, for example, $F(k)F(P-k)$, appears in the case of the pion wave function, but is absent in the case of the photon wave function $\phi_{\gamma\perp}(u,P^2)$. In the opinion of the authors of ref. [12], this end-point behavior of the transverse light-cone wave function is not conclusive, they expect that an asymptotic-like shape would be recovered in the calculation that was made with an explicit ultraviolet cutoff of order of the instanton size. However, our explicit calculation with such cutoff shows that the resultant end-point behavior still remains unchanged provided that the cutoff is large enough, and of the order of 1 GeV, close to the inverse of the instanton size.

Furthermore, we may expand the wave functions $\phi_{\gamma\perp}(u,P^2)$, $h_{\gamma\|}^{(s),\text{twist two}}(u,P^2)$ and $h_{\gamma\|}^{(t),\text{twist two}}(u,P^2)$ in the Gegenbauer polynomials for the purpose of practice:

$$\phi_{\gamma\perp}\big(u,P^2\big)=A+6u\bar{u}\sum_{n=0,2,4\ldots}a_nC_n^{3/2}(2u-1), \tag{40}$$

$$h_{\gamma\|}^{(s),\text{twist two}}\big(u,P^2\big)=6u\bar{u}\sum_{n=0,2,4\ldots}b_nC_n^{3/2}(2u-1), \tag{41}$$

$$h_{\gamma\|}^{(t),\text{twist two}}\big(u,P^2\big)= C+6u\bar{u}\sum_{n=0,2,4\ldots}c_nC_n^{1/2}(2u-1). \tag{42}$$

Table 15. Gegenbauer coefficients of $h_{\gamma\|}^{(t),\text{twist two}}(u,P^2)$ with $n=1$ and $M=350\,\text{MeV}$.

P^2 [MeV^2]	C	c_0	c_2	c_4	c_6
-500^2	5.42057	−4.45529	−0.73369	−0.17156	−0.02866
-250^2	4.98191	−4.01030	−0.60143	−0.14091	−0.02335
0	4.82882	−3.85517	−0.55640	−0.13105	−0.02152
250^2	4.67198	−3.69636	−0.51089	−0.12132	−0.01959
500^2	4.16200	−3.18129	−0.36696	−0.09025	−0.01162

Table 16. Gegenbauer coefficients of $h_{\gamma\|}^{(t),\text{twist two}}(u,P^2)$ with $n=1$ and $M=400\,\text{MeV}$.

P^2 [MeV^2]	C	c_0	c_2	c_4	c_6
-500^2	5.36034	−4.39405	−0.71517	−0.16701	−0.02783
-250^2	4.95776	−3.98589	−0.59516	−0.13975	−0.02286
0	4.81764	−3.84401	−0.55437	−0.13081	−0.02101
250^2	4.67299	−3.69770	−0.51279	−0.12171	−0.01892
500^2	4.17030	−3.19147	−0.37084	−0.08700	−0.00829

Table 17. Gegenbauer coefficients of $h_{\gamma\|}^{(t),\text{twist two}}(u,P^2)$ with $n=2$ and $M=350\,\text{MeV}$.

P^2 [MeV^2]	C	c_0	c_2	c_4	c_6
-500^2	5.40491	−4.43936	−0.72922	−0.17070	−0.02849
-250^2	5.00287	−4.03149	−0.60771	−0.14246	−0.02368
0	4.86447	−3.89120	−0.56666	−0.13339	−0.02210
250^2	4.72414	−3.74901	−0.52547	−0.12453	−0.02051
500^2	4.29317	−3.31278	−0.40179	−0.09932	−0.01563

Table 18. Gegenbauer coefficients of $h_{\gamma\|}^{(t),\text{twist two}}(u,P^2)$ with $n=2$ and $M=400\,\text{MeV}$.

P^2 [MeV^2]	C	c_0	c_2	c_4	c_6
-500^2	5.35425	−4.38781	−0.71382	−0.16701	−0.02777
-250^2	4.98648	−4.01487	−0.60386	−0.14204	−0.02335
0	4.86139	−3.88813	−0.56714	−0.13404	−0.02186
250^2	4.73509	−3.76021	−0.53043	−0.12619	−0.02032
500^2	4.34640	−3.36709	−0.41973	−0.10301	−0.01510

Table 19. Gegenbauer coefficients of $h_{\gamma\|}^{(t),\text{twist two}}(u,P^2)$ with $n=5$ and $M=350\,\text{MeV}$.

P^2 [MeV^2]	C	c_0	c_2	c_4	c_6
-500^2	5.42778	−4.46252	−0.73642	−0.17254	−0.02875
-250^2	5.02632	−4.05522	−0.61501	−0.14431	−0.02396
0	4.88906	−3.91608	−0.57420	−0.13525	−0.02240
250^2	4.75034	−3.77551	−0.53333	−0.12641	−0.02086
500^2	4.32742	−3.34730	−0.41126	−0.10143	−0.01629

Table 20. Gegenbauer coefficients of $h_{\gamma\|}^{(t),\text{twist two}}(u,P^2)$ with $n=5$ and $M=400\,\text{MeV}$.

P^2 [MeV^2]	C	c_0	c_2	c_4	c_6
-500^2	5.38152	−4.41540	−0.72248	−0.16925	−0.02804
-250^2	5.01399	−4.04267	−0.61252	−0.14429	−0.02367
0	4.89008	−3.91710	−0.57605	−0.13634	−0.02222
250^2	4.76565	−3.79106	−0.53975	−0.12859	−0.02077
500^2	4.38977	−3.41065	−0.43211	−0.10640	−0.01621

The resultant Gegenbauer coefficients of the photon wave functions, $\phi_{\gamma\perp}(u,P^2)$, $h_{\gamma\|}^{(s),\text{twist two}}(u,P^2)$ and $h_{\gamma\|}^{(t),\text{twist two}}(u,P^2)$, are shown in tables 3-20.

This work is supported by the National Natural Science Foundation of China under Grant No. 10075036, BEPC National Laboratory Project R&D and BES Collaboration Research Foundation.

Appendix A.

In this appendix, we give a derivation of the Wandzura-Wilczek–like relations which relate the other chirality-violating light-cone photon wave functions to the transverse one $\phi_{\gamma\perp}(u,P^2)$. Duo to the similarity between the Lorentz decomposition of the photon distribution amplitudes and those for the rho meson, as given in the previous section, one may conclude that there may exist similar Wandzura-Wilczek–like relations. However, an explanation for these relations to be valid should be given because such expressions are, in an essential step, derived by using the equation of motion which is modified by the existence of the electromagnetic fields. In order to make this point clearer, we will directly follow ref. [23] step by step, and rewrite down the similar formulae with some patience. First, we write the matrix elements of the operators of interest in the light-cone limit $x^2\to 0$ in terms of the photon wave functions according to the definition of eq. (1):

$$\begin{aligned}
&\langle 0|\bar\psi(x)\sigma_{\mu\nu}x^\nu[x,-x]\psi(-x)|\gamma(P,\lambda)\rangle=\\
&if_\gamma^\perp(P^2)\Big\{\left(e_\mu^{(\lambda)}-\frac{e^{(\lambda)}\cdot x}{Px}P_\mu\right)(Px)\\
&\times\int_0^1 \mathrm{d}u e^{i\xi P\cdot x}\left[\phi_{\gamma\perp}(u,P^2)+\mathcal{O}(x^2)\right]\\
&-\frac{e^{(\lambda)}\cdot x}{Px}\left(x_\mu-\frac{x^2}{Px}P_\mu\right)P^2\\
&\times\int_0^1 \mathrm{d}u e^{i\xi P\cdot x}\left[h_{\gamma\|}^{(t)}(u,P^2)-\phi_{\gamma\perp}(u,P^2)\right]\Big\},
\end{aligned}\tag{A.1}$$

$$\begin{aligned}
&\langle 0|\bar\psi(x)[x,-x]\psi(-x)|\gamma(P,\lambda)\rangle=\\
&-i\left(f_\gamma^\perp(P^2)-f_\gamma(P^2)\frac{2m_\psi\mu}{P^2}\right)(e^{(\lambda)}\cdot x)P^2\\
&\times\int_0^1 \mathrm{d}u e^{i\xi P\cdot x}\left[h_{\gamma\|}^{(s)}(u,P^2)+\mathcal{O}(x^2)\right]
\end{aligned}\tag{A.2}$$

and

$$\begin{aligned}
&\langle 0|\bar\psi(x)\not{x}[x,-x]\psi(-x)|\gamma(P,\lambda)\rangle=\\
&f_\gamma(P^2)\mu e^{(\lambda)}\cdot x\int_0^1 \mathrm{d}u e^{i\xi P\cdot x}\left[\phi_{\gamma\|}(u,P^2)+\mathcal{O}(x^2)\right]
\end{aligned}\tag{A.3}$$

based on the Lorentz covariance. Then, we need to use the following exact operator identities between the non-local operators:

$$\begin{aligned}
&\frac{\partial}{\partial x_\mu}\left\{\bar\psi(x)\sigma_{\mu\nu}x^\nu[x,-x]\psi(-x)\right\}=\\
&i\int_{-1}^1 \mathrm{d}v v\bar\psi(x)x^\alpha\sigma_{\alpha\beta}[x,vx]x^\mu gG_{\mu\beta}(vx)[vx,-x]\psi(-x)\\
&+i\int_{-1}^1 \mathrm{d}v v\bar\psi(x)x^\alpha\sigma_{\alpha\beta}[x,vx]x^\mu e_\psi F_{\mu\beta}(vx)[vx,-x]\psi(-x)\\
&-ix^\beta\partial_\beta\left\{\bar\psi(x)[x,-x]\psi(-x)\right\}
\end{aligned}\tag{A.4}$$

and

$$\begin{aligned}
&\bar\psi(x)[x,-x]\psi(-x)-\bar\psi(0)\psi(0)=\\
&\int_0^1\mathrm{d}t\int_{-t}^t\mathrm{d}v\bar\psi(tx)x^\alpha\sigma_{\alpha\beta}[tx,vx]x^\mu g\\
&\times G_{\mu\beta}(vx)[vx,-tx]\psi(-tx)\\
&+\int_0^1\mathrm{d}t\int_{-t}^t\mathrm{d}v\bar\psi(tx)x^\alpha\sigma_{\alpha\beta}[tx,vx]x^\mu Q_\psi\\
&\times F_{\mu\beta}(vx)[vx,-tx]\psi(-tx)\\
&+i\int_0^1\mathrm{d}t\partial^\alpha\left\{\bar\psi(tx)\sigma_{\alpha\beta}x^\beta[tx,-tx]\psi(-tx)\right\}\\
&+2im_\psi\int_0^1\mathrm{d}t\bar\psi(tx)\not{x}[tx,-tx]\psi(-tx),
\end{aligned}\tag{A.5}$$

where $\partial_\mu\{\}$ denotes the derivative over the total translation defined by eq. (3.3) in ref. [23]. We note that the only difference between the similar formulae here and those in [23] is the appearance of terms involving the electromagnetic field strength $F_{\mu\beta}(vx)$, because there is an additional term in the commutator: $[D_\mu,D_\nu]=-igG_{\mu\nu}-iQF_{\mu\nu}$ in consideration of the electromagnetic interactions.

Sandwiching eqs. (A.4) and (A.5) between the vacuum and the photon state, and setting $x=z$, we obtain a system of integral equations:

$$\begin{aligned}
&-i(p\cdot z)\int_0^1\mathrm{d}u e^{i\xi p\cdot z}\xi h_{\gamma\|}^{(t)}(u,P^2)\\
&-2\int_0^1\mathrm{d}u e^{i\xi p\cdot z}\left[h_{\gamma\|}^{(t)}(u,P^2)-\phi_{\gamma\perp}(u,P^2)\right]=\\
&\xi_{3\gamma}^\perp(P^2)(p\cdot z)^2\int_{-1}^1\mathrm{d}v v T_\gamma(v,p,z)\\
&+\left[1-\varrho(P^2)\right](p\cdot z)^2\int_0^1\mathrm{d}u e^{i\xi p\cdot z}h_{\gamma\|}^{(s)}(u,P^2),
\end{aligned}\tag{A.6}$$

$$\begin{aligned}
&\left[1-\varrho(P^2)\right]\int_0^1\mathrm{d}u e^{i\xi p\cdot z}h_{\gamma\|}^{(s)}(u,P^2)=\\
&i\xi_{3\gamma}^\perp(P^2)(p\cdot z)\int_0^1 t\mathrm{d}t\int_{-1}^1\mathrm{d}v T_\gamma(v,tp,z)\\
&+\int_0^1\mathrm{d}t\int_0^1\mathrm{d}u e^{i\xi tp\cdot z}h_{\gamma\|}^{(t)}(u,P^2)\\
&-\varrho(P^2)\int_0^1\mathrm{d}t\int_0^1\mathrm{d}u e^{i\xi tp\cdot z}\phi_{\gamma\|}(u,P^2)
\end{aligned}\tag{A.7}$$

with

$$\varrho\big(P^2\big)=\frac{2f_\gamma\big(P^2\big)m_\psi}{f_\gamma^\perp\big(P^2\big)\mu}\,,\qquad \xi_{3\gamma}^\perp\big(P^2\big)=\frac{f_{3\gamma}^\perp\big(P^2\big)\mu}{f_\gamma^\perp\big(P^2\big)P^2}\,. \quad \text{(A.8)}$$

We note that

$$\begin{aligned}&\Big(e^{(\lambda)}\cdot z\Big)(p\cdot z)f_{3\gamma}^\perp\big(P^2\big)\mu\int_{-1}^1 \mathrm{d}v v T_\gamma(v,p,z)=\\&\int_{-1}^1 \mathrm{d}v v\langle 0|\bar\psi(z)z^\alpha\sigma_{\alpha\beta}[z,vz]z^\alpha gG_{\mu\beta}(vz)[zx,-z]\\&\times\psi(-z)|\gamma(P,\lambda)\rangle+Q_\psi\int_{-1}^1 \mathrm{d}v v\langle 0|\bar\psi(z)z^\alpha\sigma_{\alpha\beta}[z,vz]z^\alpha\\&\times F_{\mu\beta}(vz)[zx,-z]\psi(-z)|\gamma(P,\lambda)\rangle,\end{aligned}\quad \text{(A.9)}$$

where the last term in the r.h.s. vanishes because

$$\begin{aligned}&\langle 0|\bar\psi(z)\sigma_{\alpha\beta}[z,vz]F_{\mu\rho}(vz)[zx,-z]\psi(-z)|\gamma(P,\lambda)\rangle=\\&i\int \mathrm{d}^4x e_\nu^{(\lambda)}e^{-iP\cdot x}\langle 0|T\big\{\bar\psi(z)\sigma_{\alpha\beta}[z,vz]F_{\mu\rho}(vz)[zx,-z]\,,\\&\psi(-z)j^\nu_{\mathrm{em}}(x)\big\}|0\rangle=\\&\langle 0|\bar\psi(z)\sigma_{\alpha\beta}[z,vz]F_{\mu\rho}(vz)[zx,-z]\psi(-z)|0\rangle_F=0\end{aligned}\quad \text{(A.10)}$$

with the understanding for $\langle 0|O(z)|\gamma(P,\lambda)\rangle$ being described in eq. (1), and $\langle 0|O(z)|0\rangle_F$ the vacuum expectation value of the operator $O(z)$ in the external electromagnetic background fields. Therefore, eqs. (6) and (7) are, in fact, the same as eqs. (3.6) and (3.7) in [23]. Then, it is obvious that the same consequence as in [23] can be obtained in the same straightforward way. In particular, the wave functions $h_{\gamma\|}^{(t)}$ and $h_{\gamma\|}^{(s)}$ receive contributions of both leading-twist two and non-leading twist three, and the twist-two contributions are related to the transverse distribution $\phi_{\gamma\perp}$ by Wandzura-Wilczek–like relations, eqs. (5) and (6) [30].

References

1. S.J. Brodsky, G.P. Lepage, in *Perturbative Quantum Chromodynamics*, edited by A.H. Mueller (World Scientific, Singapore, 1989) p. 93.
2. G.P. Lepage, S.J. Brodsky, Phys. Lett. B **87**, 359 (1979); Phys. Rev. Lett. **43**, 545 (1979); **43**, 1625 (1979)(E); Phys. Rev. D **22**, 2157(1980).
3. A.V. Efremov, A.V. Radyushkin, Phys. Lett. B **94**, 425 (1980).
4. V.L. Chernyak, A.R. Zhitnisky, JETP Lett. **25**, 510 (1977); Yad. Fiz. **31**, 1053 (1980).
5. V.M. Braum, hep-th/9801222.
6. I.I. Balitsky, V.M. Braum, A.V. Kolesnichenko, Nucl. Phys. B **312**, 509 (1989).
7. A.V. Radyushkin, R. Ruskov, Phys. Lett. B **374**, 173 (1996); Nucl. Phys. B **481**, 625 (1996).
8. A.V. Radyushkin, Phys. Lett. B **380**, 417 (1996); **385**, 333 (1996).
9. X. Ji, Phys. Rev. Lett. **78**, 610 (1997); Phys. Rev. D **55**, 7114 (1997).
10. CLEO Collaboration (J. Gronberg *et al.*), Phys. Rev. D **57**, 33 (1998).
11. V.L. Chernyak, A.R. Zhitnisky, Phys. Rep. **112**, 173 (1984).
12. Patricia Ball, V.M. Braun, N. Kivel, Nucl. Phys. B **649**, 263 (2003).
13. V.V. Anisovich, D.I. Melikhov, V.A. Nikonov, Phys. Rev. D **55**, 2918 (1997).
14. J.C. Collins, L. Frankfurt, M. Strikman, Phys. Rev. D **56**, 2989 (1997).
15. L. Mankiewicz, G. Piller, T. Weigl, Eur. Phys. J. C **5**, 119 (1998).
16. D. Diakonov, V. Petrov, Nucl. Phys. B **272**, 457 (1986); D.I. Diakonov, talk given at the *International School of Physics Enrico Fermi, Varenna, Italy, 1995, Course CXXX, Selected Topics in Nonperturbative QCD Vacuum*, hep-ph/9602375.
17. M. Shifman, A. Vainstein, V. Zakharov, Nucl. Phys. B **147**, 385 (1979).
18. J.P. Liu, Y.P. Jin, Jian Ze, Z. Phys. C **59**, 313 (1993).
19. G. 't Hooft, Phys. Rev. Lett. **37**, 8 (1976); Phys. Rev. D **14**, 3432 (1976); **18**, 2199 (1978)(E).
20. D. Diakonov, *The $U(1)$ problem and instantons*, in *Gauge Theories of the Eighties*, Lect. Notes Phys., Vol. **181** (Springer-Verlag, 1983) p. 127.
21. D. Diakonov, V. Petrov, *Diquark in the instanton picture*, in *Quark Cluster Dynamics*, Lect. Notes Phys., Vol. **417** (Springer-Verlag, 1992) p. 288.
22. V.Yu. Petrov, M.V. Polyakov, R. Ruskov, C. Weiss, K. Goeke, Phys. Rev. D **59**, 114018 (1999).
23. Patricia Ball, V.M. Braun, Y. Koike, K. Tanaka, Nucl. Phys. B **529**, 323 (1998).
24. Patricia Ball, V.M. Braun, Phys. Rev. D **54**, 2182 (1996).
25. Ran Yu, Jueping Liu, Kai Zhu, Phys. Rev. D **73**, 045002 (2006); Chin. Phys. Lett. **22**, 2515 (2005).
26. Michal Praszalowicz, Andrzej Rostworowski, Phys. Rev. D **64**, 074003 (2001).
27. S.J. Brodsky, G.P. Lepage, Phys. Rev. D **22**, 2157 (1980); L.I. Balitsky, V.M. Braun, Nucl. Phys. B **311**, 541 (1988/89).
28. Zhu Kai, Liu Jueping, Yu Ran, Chin. Rev. Lett. **23**, 1128 (2006).
29. V.L. Chernyak, A.R. Zhitnisky, Phys. Rep. **112**, 173 (1984).
30. S. Wandzura, F. Wilczek, Phys. Lett. B **72**, 195 (1977).
31. D.I. Diakonov, V.Yu. Petrov, Nucl. Phys. B **245**, 259 (1984).